Received: 18 January 2018 | Revised: 29 June 2018 | Accepted: 2 July 2018

DOI: 10.1002/hbm.24313

WILEY

RESEARCH ARTICLE

Functional cerebral asymmetry analyses reveal how the control system implements its flexibility

Zhencai Chen[1] | Xiaoyue Zhao[2] | Jin Fan[3,4,5] | Antao Chen[2]

[1]Department of Psychology, Jiangxi University of Traditional Chinese Medicine, Nanchang, China

[2]Key Laboratory of Cognition and Personality of Ministry of Education, Faculty of Psychology, Southwest University, Chongqing, China

[3]Department of Psychology, Queens College, The City University of New York, Icahn School of Medicine at Mount Sinai, New York City, New York

[4]Department of Psychiatry, Icahn School of Medicine at Mount Sinai, New York City, New York

[5]Department of Neuroscience, Icahn School of Medicine at Mount Sinai, New York City, New York

Correspondence
Antao Chen, Faculty of Psychology, Southwest University, Chongqing 400715, China.
Email: xscat@swu.edu.cn

Funding information
Research Foundation of Jiangxi University of Traditional Chinese Medicine, Grant/Award Number: 5151700708; National Natural Science Foundation of China, Grant/Award Numbers: 61431013, 31771254; Fundamental Research Funds for the Central Universities, Grant/Award Numbers: SWU1609106, SWU1709107

Abstract

The control system in human brain generally exerts the goal-directed regulation on a variety of mental processes. To deal with different control demands, these brain areas of the control system, especially the dorsolateral prefrontal cortex (DLPFC), may be flexibly recruited across different tasks. However, few studies have investigated how the flexibility of the control system is realized during cognitive control. Present study employed functional magnetic resonance imaging to examine the brain responses during two domain distinct conflict tasks (verbal color-word Stroop and visuospatial arrow flanker). The voxel-wise asymmetries in both functional activity and psychophysiological interaction (PPI) between these two tasks were compared. The results showed that the brain areas of control system were consistently activated in these two tasks. When considering functional cerebral asymmetries, the left DLPFC was dominantly activated during the Stroop task, while more symmetric DLPFC activation was found during the flanker task. The left DLPFC rather than the right DLPFC showed greater positive interaction with the visual areas V1 and V2 during the Stroop interference, but interactions of both the left and right DLPFC with the right visual area V5/MT were positively enhanced during the flanker interference. These results suggest that the flexible cognitive control is achieved by the control system's task-specific activity and its top–down interaction with domain-specific brain areas, in implementing flexible representation and modulation of control demands.

KEYWORDS

control flexibility, control system, dorsolateral prefrontal cortex, fMRI, functional cerebral asymmetry, psychophysiological interaction

1 | INTRODUCTION

Through implementing goal-directed guidance, cognitive control supervises, and regulates a variety of cognitive processes (Fan, 2014; Spagna, Mackie, & Fan, 2015). As a general cognitive function, the cognitive control involves four hierarchical processes: the stimulus perception, salience detection, goal-directed regulation, and response selection. In addition to these general cognitive control functions, different cognitive control tasks which have different stimulus features, goals, and response rules (i.e., task sets) (Sakai, 2008), would induce flexible task-specific control processing. Thus, the cognitive control is embodied in task-general and -specific responding to various task demands (Braver, Paxton, Locke, & Barch, 2009; Cole et al., 2013). However, the exact neural mechanisms of how multiple cognitive control demands are represented and how the flexible cognitive control is performed in the brain are still unclear.

Cognitive control is subserved by a control system of the human brain, that is, the cognitive control network (CCN), which includes the frontoparietal network (FPN) and the cingulo-opercular network (CON) and exerts adaption to multiple tasks (Cole & Schneider, 2007; Miller & Cohen, 2001; Wu et al., 2017). Apart from the task-general regions of control system (e.g., the midcingulo-insular-inferior frontal core network) (Cieslik, Mueller, Eickhoff, Langner, & Eickhoff, 2015), one core region for flexible task-specific cognitive control is the dorsolateral prefrontal cortex (DLPFC) (Braver et al., 2009; Cole et al., 2013). The DLPFC cooperates with other brain regions (e.g., the anterior cingulate cortex (ACC), the posterior parietal cortex (PPC), and stimulus-input and response-output regions), to represent task rule, allocate attentional resources, resolve conflict, and flexibly modulate a large set of cognitive functions (Botvinick, Braver, Barch, Carter, & Cohen, 2001; Braun et al., 2015; Fan, Hof, Guise, Fossella, & Posner, 2008). Therefore, the flexible control functions of DLPFC, which may

include the DLPFC's flexible activation and top-down modulation, should reflect how the control system is engaged in various task demands. In the present study, we aimed to further clarify the neural mechanisms of how the flexibility of cognitive control is achieved by the DLPFC's functional architectures.

To investigate this issue, cognitive control tasks with distinct control system processes in addition to the task-general cognitive control were needed. We found the color-word Stroop task and arrow flanker task (Eriksen & Eriksen, 1974; Fan, McCandliss, Sommer, Raz, & Posner, 2002; Stroop, 1935) are suitable for our aims. It is well known that the color-word Stroop task needs word-verbal processing and the arrow flanker task may need direction-spatial processing. These two typical paradigms in cognitive control studies involve different task sets, which may evoke different control demands. When solving these different conflicts, the flexible cognitive control processing of DLPFC may task-specifically activate and interact with those areas responsible for the specialized word and direction processes.

Notably, the functional cerebral asymmetry (FCA) activity is a basic feature of cerebral functions, especially for verbal and visuospatial processes (Hugdahl & Davidson, 2004; Hugdahl & Westerhausen, 2010), which are recruited in the color-word Stroop and arrow flanker tasks. In fact, FCA activity has been observed in the Stroop task. Specifically, the inhibition of DLPFC to the task-irrelevant word reading during the Stroop task is associated with the left hemispheric lateralization of language processing, for instance the left DLPFC shows more instantaneous response and intensive activity than the right DLPFC to suppress the task-irrelevant word reading processing (Hugdahl & Davidson, 2004; Leung, Skudlarski, Gatenby, Peterson, & Gore, 2000; Ye & Zhou, 2009). Presumably, the task-specific FCA activity could also be observed in the flanker task. If so, the lateralization result can suggest how the control system can flexibly represent and respond to various cognitive control demands. Additionally, cognitive control also relies on large-scale interactions between DLPFC and other brain regions (Cocchi, Zalesky, Fornito, & Mattingley, 2013). The functional connectivity based on the DLPFC is related to the attention to endogenous events and changes as a function of control complexity (Bressler & Menon, 2010; Dosenbach, Fair, Cohen, Schlaggar, & Petersen, 2008). Thus, the task-specific functional connectivity of DLPFC should also be investigated to reveal how the control system interacts with other brain areas to flexibly handle different control demands.

In this study, we employed fMRI to investigate functional activity and connectivity of the DLPFC during the color-word Stroop and arrow Eriksen flanker tasks. We used the activation contrast, conjunction null hypothesis (Friston, Penny, & Glaser, 2005; Nichols, Brett, Andersson, Wager, & Poline, 2005), and voxel-wise asymmetry analyses (Stevens, Calhoun, & Kiehl, 2005) to examine the flexible cerebral representation of cognitive control, and the psychophysiological interaction (PPI) and functional connectivity lateralization index (FCLI) analyses (Di, Kim, Chen, & Biswal, 2014; Friston et al., 1997; O'Reilly, Woolrich, Behrens, Smith, & Johansen-Berg, 2012) were performed to further reveal the adaptive interaction between the DLPFC and the other brain regions for different cognitive demands. The task-specific representation and modulation of the control system may shed light on the mechanisms of flexible cognitive control.

2 | MATERIALS AND METHODS

2.1 | Participants

Two groups of college students, 38 for the Stroop task (22 females; mean age = 21.31 years, *SD* = 1.95) and 38 for the flanker task (18 females; mean age = 21.80 years, *SD* = 1.79), were recruited in this study. All participants were right-handed, had normal or corrected to normal vision and normal color perception, and received monetary compensation for their participation. The Stroop task data of two participants and flanker task data of three participants were excluded due to head motion (>2.5 mm or 2.5°). The study was approved by the Human Ethics Committee for Brain Mapping Research at Southwest University, China and a written consent was obtained from each participant before the experiment.

2.2 | Experimental paradigms

A 4–2 mapping Stroop task (Chen, Lei, Ding, Li, & Chen, 2013; De Houwer, 2003) was employed using four Chinese characters of "Red," "Yellow," "Blue," and "Green" on a black background (see Figure 1 top panel). Each character was presented in one of the four colors (i.e., red, yellow, blue, and green; 16 stimuli altogether). Participants were asked to respond according to the colors of the characters; the red and yellow colors were mapped onto the thumb of the left hand, while the blue and green colors were mapped onto the thumb of the right hand. There were three types of stimuli: congruent stimuli (CO, e.g., "Red" word in red), semantic incongruent stimuli (SI, e.g., "Red" word in yellow) and response incongruent stimuli (RI, e.g., "Red" word in blue). Note that, because the RI–CO contrast represented the total Stroop interference effect and the semantic incongruent was contaminated by semantic and response interference effects (Chen et al., 2013), for further analyses, the RI rather than the SI condition was regarded as the incongruent condition (IC) to define the Stroop interference effect (IC–CO). In total, 120 trials of two runs were employed in this study, which consisted of 48 congruent trials, 36 semantically incongruent trials, and 36 response incongruent trials. We used this relatively higher ratio of CO to SI + RI trials (i.e., 1:1.5) than 1:2 (i.e., CO:SI:RI as 1:1:1) to reduce the expectancy of conflict and to maintain the Stroop effect (Carter et al., 2000; Fellows & Farah, 2005; Van Veen & Carter, 2005). Stimuli were presented at pseudo-random order with no more than three repeated responses made.

For the flanker task, the stimulus was a row of five black single-head arrows on a gray background (see Figure 1 bottom panel), with arrowhead pointed to left or right as in a previous study (Fan et al., 2002; Fan, McCandliss, Fossella, Flombaum, & Posner, 2005). The visual angle was controlled with each arrow subtended 0.58° of visual angle and separated by 0.06° of visual angle, the stimuli (five arrows) subtended a total 3.27° of visual angle. The center target (leftward or rightward arrow) was flanked by the peripheral arrows with the same (CO) or opposite (IC) direction. Participants were asked to press the left key with the thumb of left hand when the central arrow was leftward, and pressing the right key with the thumb of the right hand when the central arrow was rightward. A total of 160 trials of two runs were performed in this study, in which each run consisted of

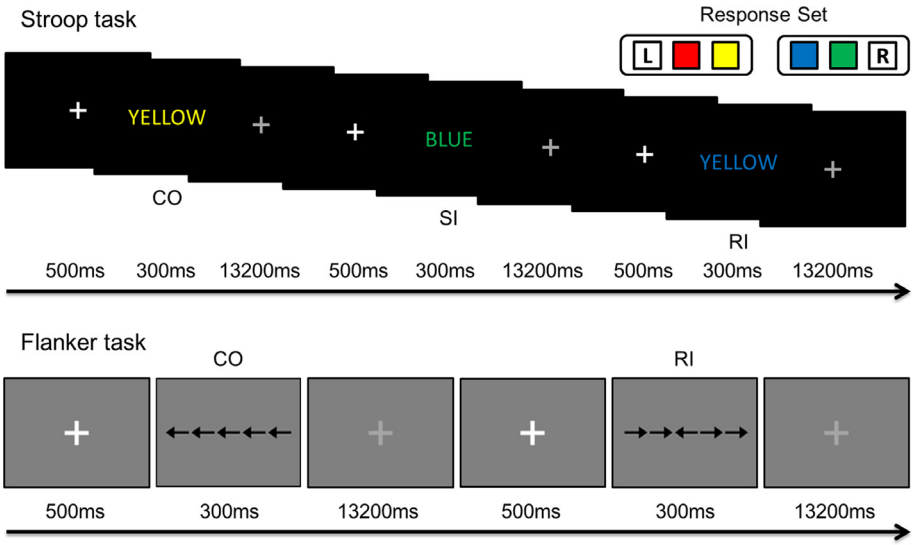

FIGURE 1 Behavioral protocols of Stroop and flanker tasks. In the top panel, the Chinese character "yellow" and the Chinese character "blue" were displayed in the same or different colors and response sets to their word meanings. The Stroop task contained congruent (CO), semantic incongruent (SI), and response incongruent (RI) stimuli. In the bottom panel, the flanker task contained CO and RI conditions [Color figure can be viewed at wileyonlinelibrary.com]

40 congruent trials and 40 incongruent trials in a pseudo-random order.

The trials in both the Stroop and flanker tasks started with a white fixation for 500 ms, and after the characters or arrows had been displayed for 300 ms, there was a gray fixation for a 1,200 ms response period, and then followed by an additional 12,000 ms gray fixation as the inter-trial interval. The extended interval time between the stimuli allowed the blood-oxygen-level dependent (BOLD) signal to return to baseline, which can improve the detection of brain activation and PPI neural signal deconvolution (Bandettini & Cox, 2000).

2.3 | Behavioral data analysis

Behavioral interference effects of Stroop and flanker tasks were calculated as the difference between mean reaction time (RT) of CO and IC conditions (IC–CO). Error trials and trials longer than 1,500 ms or shorter than 300 ms in RT were excluded. A one-sample *t*-test was conducted to test the interference effect (difference between the CO and IC) in RT.

2.4 | Image acquisition and preprocessing

Images were acquired with a Siemens 3 T scanner (Siemens Magnetom Trio TIM, Erlangen, Germany). An echo-planar imaging (EPI) sequence was used for data collection of functional images (repetition time = 2,000 ms; echo time = 30 ms; flip angle = 90°; field of view = 220 × 220 mm^2; matrix size = 64 × 64; 32 interleaved 3 mm-thick slices; in-plane resolution = 3.4 × 3.4 mm^2; inter-slice skip = 0.99 mm). There were 432 and 292 EPI images recorded per run for Stroop and flanker tasks, respectively. T1-weighted images were also recorded with a total of 176 slices with a 1 mm thickness and a 0.98 × 0.98 mm^2 in-plane resolution (TR = 1,900 ms; TE = 2.52 ms; flip angle = 9°; FoV = 250 × 250 mm^2).

We used SPM8 (Wellcome Department of Cognitive Neurology, London, The United Kingdom, http://www.fil.ion.ucl.ac.uk/spm/spm8) to pre-process the EPI images (Friston, Holmes, et al., 1994). The first five images were discarded, and then the slice timing correction was conducted. Through estimating (the first volume as a reference) and using a 6-parameter rigid-body spatial transformation matrix, the EPI images were realigned to correct the head movement. These head movement corrected EPI images were then normalized to Montreal Neurological Institute (MNI) EPI template in 3 × 3 × 3 mm^3 voxel size. The normalized images were spatially smoothed with a Gaussian kernel with the full width at half maximum as 8 × 8 × 8 mm^3.

2.5 | Activation analyses

Using SPM8, two general linear models (GLM) were estimated. In the GLM for Stroop task, four regressors (i.e., congruent, semantic incongruent, response incongruent, and error) were included for each run in the design matrix. Regressors were convolved with the canonical hemodynamic response function (Friston, Jezzard, & Turner, 1994) and the six realignment parameters were included as covariates (Friston, Williams, Howard, Frackowiak, & Turner, 1996). The contrast of IC–CO was defined for the Stroop interference effect. In the GLM for the flanker task, three regressors (i.e., congruent, incongruent, and error) were included for each run, and the flanker interference contrast (IC–CO) was also defined. Next, the group activation analyses were performed with random effect models. Finally, the interference effect difference between Stroop and Flanker tasks was examined by a two-sample *t*-test, and their common activation was examined by a conjunction analysis which is based on conjunction null hypothesis (Friston et al., 2005; Nichols et al., 2005). Gender and age factors were regressed out as covariates during these analyses. The group effects were corrected with a voxel-wise height of $p < .001$ and a cluster family-wise error (FWE) of $p < .05$ for multiple comparisons

(Forman et al., 1995; Friston, Worsley, Frackowiak, Mazziotta, &, Evans, 1994).

2.6 | Asymmetry activation calculation

To investigate the distinct FCA activity of Stroop and flanker tasks, the voxel-wise asymmetry algorithm (Stevens et al., 2005) was used to calculate the asymmetry maps to avoid the threshold sensitiveness problem of voxel counting while computing a laterality index (Swanson et al., 2011). To deal with the structure differences between left and right cerebral hemispheres, we first created a hemispherically symmetric EPI template by averaging the MNI EPI template and its left–right flipped image. Then for each participant, we registered the original spatially normalized mean EPI images to this symmetric EPI template, and used the coregistration parameters to normalize the Stroop and flanker interference contrast images from the above GLMs. Laterality User Interface (LUI) software (http://mialab.mrn.org/software/) was used to generate the Left–Right image (i.e., the right hemisphere is the mirror of left hemisphere) and Right–Left image (i.e., the left hemisphere is the mirror of right hemisphere). Finally, the LUI subtracted the Right–Left image from the Left–Right image at the voxel-wise level to compute asymmetry maps of Stroop and flanker interference activations (Stevens et al., 2005). The group asymmetry effects were tested using a one-sample *t*-test, with a significant level of $p < .001$ voxel-wise and $p < .05$ cluster-wise FWE correction.

2.7 | Interregional interactions from bilateral DLPFCs

The PPI analysis was conducted to indicate the regions that showed significantly different correlations with the seed region (e.g., DLPFC) under different conditions (e.g., CO and IC in our study) (Friston et al., 1997; O'Reilly et al., 2012). In other words, the PPI regressor predicted the effects of an experimental factor on the target region when taking the input from the source region into consideration. Based on the group activation of interference effects, we defined spherical regions of interest (ROIs) with a radius of 6 mm and maximum peaks within the anterior and middle third (centered at the junction between Brodmann's area [BA] 9 and BA 46) of the bilateral middle frontal gyrus (MFG) (Mylius et al., 2013) as the coordinates of DLPFCs for Stroop (left DLPFC [lDLPFC]: −42, 29, 25; right DLPFC [rDLPFC]: 48, 32, 22), and flanker (lDLPFC: −33, 47, 16; rDLPFC: 30, 47, 7) tasks, respectively.

The PPI analyses were performed with the following steps (Friston et al., 1997): First, the time courses of these seed regions were extracted for each run as the volumes of interest (VOIs). These raw time courses were adjusted by the *F*-contrasts of congruent and incongruent conditions (effects of interest) to rule out the main effect of task. Then, the PPI parameters of the experimental contrast (IC–CO) were calculated. Lastly, these PPI parameters were entered into GLMs as the regressors to find the regions which showed significant correlations with the interaction between the physiological signal (from the lDLPFC or rDLPFC) and the psychological context of the conflict levels (CO and IC). The total PPI effects of bilateral DLPFCs were calculated using a one-sample *t*-test which integrating and testing the PPI weight images of both the lDLPFC and rDLPFC in one GLM ($p < .001$ voxel-wise and $p < .05$ cluster-wise FWE correction). Within the small volume of this total PPI effects, the group PPI results for each lateral DLPFC were tested using the one-sample *t*-test, with a significant level of $p < .001$ voxel-wise and $p < .05$ cluster-wise FWE correction.

2.8 | Functional connectivity lateralization of PPIs

The asymmetric PPIs from bilateral DLPFCs were investigated to further examine the task-specific functional connectivity of the DLPFC in cognitive control. PPI differences between the lDLPFC and rDLPFC were tested using the functional connectivity lateralization index (FCLI) map to reveal the FCA PPIs of DLPFC in the large-scale interregional interactions level with the equation (Di et al., 2014):

$$\mathrm{FCLI} = \frac{(\mathrm{LL} - \mathrm{RL}) - (\mathrm{RR} - \mathrm{LR})}{|\mathrm{LL}| + |\mathrm{LR}| + |\mathrm{RR}| + |\mathrm{RL}|}$$

Specifically, according to the above-mentioned LUI software (Stevens et al., 2005), the "LL" is the Left–Right image of lDLPFC PPIs image; the "RL" is the Left–Right image of rDLPFC PPIs image; the "RR" is the Right–Left image of rDLPFC PPIs image; and the "LR" is the Right–Left image of lDLPFC PPIs image (see Figure 4c). After this step, we created a FCLI map for each participant. The group effects were tested using a one-sample *t*-test. Since the obvious difference between Stroop and flanker tasks was in the stimulus perception level (Egner & Hirsch, 2005), then we were interested in the FCLI of PPIs in the visual cortex. Thus, the group FCLI effects were $p < .001$ voxel-wise and $p < .05$ cluster-wise FWE corrected with a small volume correction in an anatomical mask that included the occipital, occipitotemporal (i.e., inferior and middle temporal gyri) and occipitoparietal (i.e., inferior parietal lobule) cortexes (Dunst, Benedek, Koschutnig, Jauk, & Neubauer, 2014; Schultz & Cole, 2016).

The common PPIs of bilateral DLPFCs were calculated using conjunction analyses based on the conjunction null hypothesis to reveal bilateral DLPFCs' symmetric interactions with other brain regions (Friston et al., 2005; Nichols et al., 2005). The conjunction results were corrected using a small volume correction within the intersection of the above-mentioned visual cortex mask and the regions of the total PPI effects ($p < .001$ voxel-wise and $p < .05$ cluster-wise FWE correction). In addition, the PPI beta values were extracted from 6 mm radius spherical ROIs of maximum FCLI and conjunction peak coordinates for each lateral DLPFC to intuitively present the PPI differences between the bilateral DLPFCs connectivity under the Stroop and flanker tasks.

3 | RESULTS

3.1 | Behavioral Stroop and flanker interference effects

For the Stroop task, the average response time of CO was significantly faster ($t[22] = 5.48$, $p < .001$) and more accurate ($t[22] = 3.22$, $p < .01$) than that of IC (reaction time [CO vs. IC], accuracy [CO vs. IC] respectively), indicating the existence of Stroop interference effect.

TABLE 1 Behavioral descriptive statistics for Stroop and flanker tasks

Task types	Congruency	Incongruency
Stroop		
Response time/CI (ms)	604 [593, 616]	665 [653, 676]
Accuracy/CI (%)	95.20 [94.21, 96.19]	93.00 [92.00, 93.98]
Interference effect/ CI (ms)	60 [49, 72]	
Flanker		
Response time/CI (ms)	493 [488, 498]	569 [564, 574]
Accuracy/CI (%)	98.93 [98.09, 99.76]	94.40 [93.59, 95.26]
Interference effect/ CI (ms)	76 [71, 81]	

CI = lower and upper bound of 95% confidence interval (Cousineau, 2005).

For the flanker task, the average response time of CO was also significantly faster (t[34] = 16.05, p < .001) and more accurate (t[34] = 5.54, p < .001) than that of IC, indicating the existence of flanker interference effect. The behavioral descriptive statistics for these tasks were presented in Table 1.

3.2 | Task-general and specific interference activation

The interference effects of the Stroop and flanker tasks were calculated in comparing with previous studies on cognitive control. Through the contrast of IC and CO conditions of the Stroop task, increased activation was found in the control system [DLPFC, dorsal anterior cingulate cortex and pre-supplementary motor area (dACC and pSMA), anterior insula and frontal operculum (aI and fO) and posterior parietal cortex (PPC)] (see Figure 2a; Table 2). Similarly, the flanker interference was associated with increased activation in the control system regions, and decreased activation in the DMN regions (see Figure 2b; Table 2).

Importantly, in present study, the common interference-related activation of the two tasks were found in the dACC and pSMA, aI and fO, and left PPC (see Figure 2c; Table 2). Meanwhile, the difference activation between Stroop and flanker tasks in interference effect was found in the left DLPFC and right PPC. Specifically, the Stroop interference caused greater activation in the left DLPFC than the flanker interference (see Figure 2d; Table 2).

3.3 | Task-specific asymmetric interference activation

The voxel-wise asymmetric activation analyses to directly compare the activation differences between the bilateral DLPFCs showed positive lateral activation in the left DLPFC, left PPC, and left temporal lobe (see Figure 3a; Table 3). For the flanker task the positive lateral FCA activity were observed in the right dACC and pSMA and aI and fO, and the negative FCA activity in the right temporal lobe (see Figure 3b; Table 3). The positive FCA activity indicates the region showed left lateralization during cognitive control, while the negative FCA activity indicates the region was right lateralized.

3.4 | Task-specific modulations of bilateral DLPFCs

The total PPI effects showed significant interactions of the bilateral DLPFCs with the visual areas during the Stroop task (see Figure 4a; Table 4), and with the SMA, primary somatosensory and motor cortex, PPC, precuneus, and visual cortex during the flanker task (see Figure 5a;

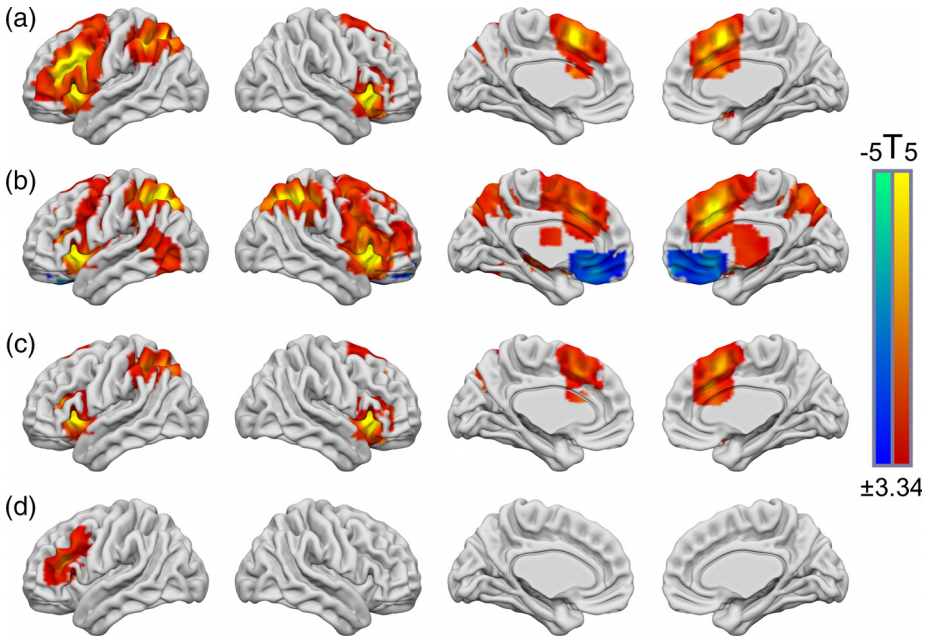

FIGURE 2 The task-dependent brain activation of interference effects. (a) The brain activation of IC–CO contrast for Stroop and (b) flanker tasks. Both of them showed activation in the task positive networks (mainly in the fronto-parietal network). The warm and cool colors meant the significantly positive and negative activation according to the IC–CO contrast. (c) The common activation of Stroop and flanker interferences through a conjunction null hypothesis analysis. (d) The different activation between Stroop and flanker interference effects (i.e., the task-dependent activation) [Color figure can be viewed at wileyonlinelibrary.com]

TABLE 2 Cerebral activations of the Stroop and flanker interference effects, and their different and conjunct activations

Region	BA	No. voxels	Peak *t*-value	*x*	*y*	*z*
Stroop						
L. Middle/inferior frontal gyrus/insula	9/46/13	1,365	7.12	−42	29	25
R. inferior frontal gyrus/insula	47/13	403	6.49	33	23	−5
Superior/medial frontal/cingulate gyrus	6/32/8	634	5.87	6	14	49
L. Superior/inferior parietal lobule	40/7	538	6.11	−30	−67	49
Flanker						
L. Inferior/middle/superior frontal gyrus/insula	6/9	550	7.38	−30	20	10
R. Inferior/middle/superior frontal gyrus/insula	6/9	1,240	7.72	33	29	4
L. Middle/inferior frontal gyrus	6	201	4.54	−15	2	46
Superior frontal/cingulate gyrus	32/6	859	6.88	9	20	40
Medial frontal/anterior cingulate gyrus	11/10	196	−4.84	0	23	−8
Thalamus/putamen		211	5.12	15	−13	10
L. Inferior/superior parietal lobule/Precuneus	7/40	674	6.52	−24	−64	52
R. Inferior/superior parietal lobule/Precuneus	7/40	764	8.23	33	−52	46
L. Inferior/middle temporal gyrus	39/37	91	4.17	−45	−67	−5
Stroop and flanker conjunction						
L. Inferior frontal gyrus/insula	13/47	324	6.21	−33	20	1
R. Inferior frontal gyrus/insula	47/13	404	6.62	33	20	−2
Superior/medial frontal/cingulate gyrus	32/6/8	480	5.19	6	17	49
L. Superior/inferior parietal lobule	40/7	365	5.73	−27	−64	46
Stroop > flanker						
L. Middle/inferior frontal gyrus	9/46	172	4.95	−42	29	19

Table 5). For unilateral DLPFCs, the PPI results showed that the DLPFC's modulations on stimulus input regions are occurred in both tasks (see Figures 4b and 5b,c; Tables 4 and 5). The positive PPI signal indicated a region had significantly more correlation with DLPFC under IC condition than that of CO condition, which demonstrated the modulation of DLPFC according to control demands.

To quantity the PPI lateralization from bilateral DLPFCs, with the FCLI map and ROI signal analysis, we found that when under the Stroop interference context the interactions of lDLPFC with the left and right visual area V1 and V2 were significant more positive (i.e., lDLPFC lateralized) than that of the rDLPFC (see Figure 4d,e; Table 4). Meanwhile, there were no common interaction regions of lDLPFC and rDLPFC according to the conjunction analysis. While for the flanker task, no significant FCLI cluster was found to bilateral DLPFCs. According to the conjunction and ROI signal analyses, both left and right DLPFCs positively interacted with the right visual area V5/MT (middle temporal, BA 37, see Figure 5d,e; Table 5).

4 | DISCUSSION

The functions of control system are thought to be generally assessed across various task demands (Buckner & Vincent, 2007; Spagna et al., 2015). In present study, with FCA activity and connectivity analyses and the original combination of the FCLI and PPI techniques, our

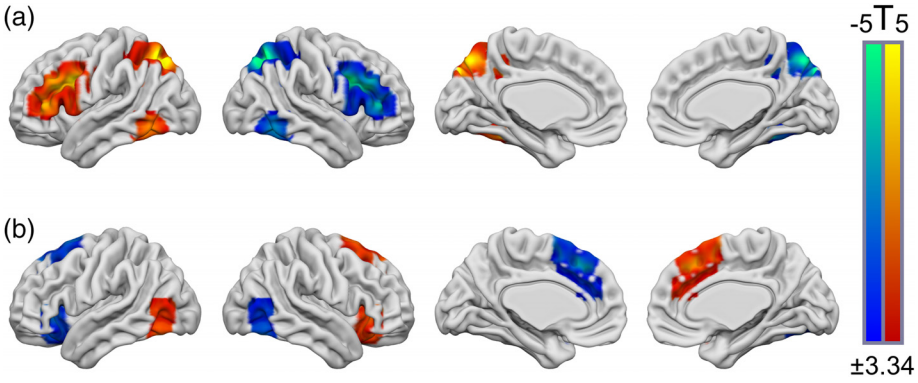

FIGURE 3 The lateral activation of interference effect. (a) The voxel-wise asymmetry activity maps for Stroop interference, which dominantly activated the left lateral fronto-parietal network; and (b) the flanker interference, which dominantly activated the right salience and cingulo-opercular networks. Note that the positive activation meant this region was in the dominant hemisphere, and vice versa [Color figure can be viewed at wileyonlinelibrary.com]

TABLE 3 Lateral brain activations for the contrasts of IC vs. CO conditions

Region	BA	No. voxels	Peak *t*-value	*x*	*y*	*z*
Stroop						
L. Middle/inferior frontal gyrus	9/44	417	5.77	−39	8	31
L. Superior/inferior parietal lobule/middle temporal gyrus	7/40/39	368	7.90	−27	−67	49
L. Inferior temporal/fusiform gyrus	37/22	72	5.37	−45	−55	−11
Flanker						
R. Superior/medial frontal gyrus/cingulate gyrus	32/6/8	247	5.12	3	29	46
R. Inferior frontal gyrus	47	47	4.89	33	32	−8
R. Middle temporal/middle occipital gyrus	37	48	−4.44	39	−70	4

results reveal the control system's flexible representation and modulation mechanisms for adaptive cognitive control. Specifically, the flexible representation of cognitive control was mainly reflected by the task-specific FCA activation of the control system, and the flexible modulation of cognitive control was reflected by the DLPFC's task-specific PPI and FCLI. Based on previous studies of flexible control system (Cocchi, Halford, et al., 2013; Dosenbach et al., 2006; Harding, Yücel, Harrison, Pantelis, & Breakspear, 2015; Menon & Uddin, 2010), present findings provide additional empirical evidence of how the multiple cognitive control demands are represented and manipulated in the human brain.

The positive activation in the control system showed a typical pattern of Stroop and flanker effects (Fan et al., 2005; Laird et al., 2005), and the deactivation in the DMN may indicate its role in facilitating the processing of internal mental noise during cognitive control (Bressler & Menon, 2010; Liu et al., 2015). Among the control system, the dACC is related to the detection of conflict (Botvinick et al., 2001; Botvinick, Cohen, & Carter, 2004), and the aI and fO is thought to evaluate task performance and monitor error response (Eckert et al., 2009; Ham, Leff, de Boissezon, Joffe, & Sharp, 2013), both of them are contained in the salience network (SN) and cingulate–opercular network (CON) which respond to salience detection and task set maintenance (Cocchi, Zalesky, et al., 2013; Dosenbach et al., 2006; Ham, Leff, de Boissezon, Joffe, & Sharp, 2013; Menon & Uddin, 2010). Meanwhile, the PPC has a function in bias relevant task representation and stimulus–response association (Brass, Ullsperger, Knoesche, Cramon, & Phillips, 2005; Harding et al., 2015). In our conjunction analysis, these regions were found to generally

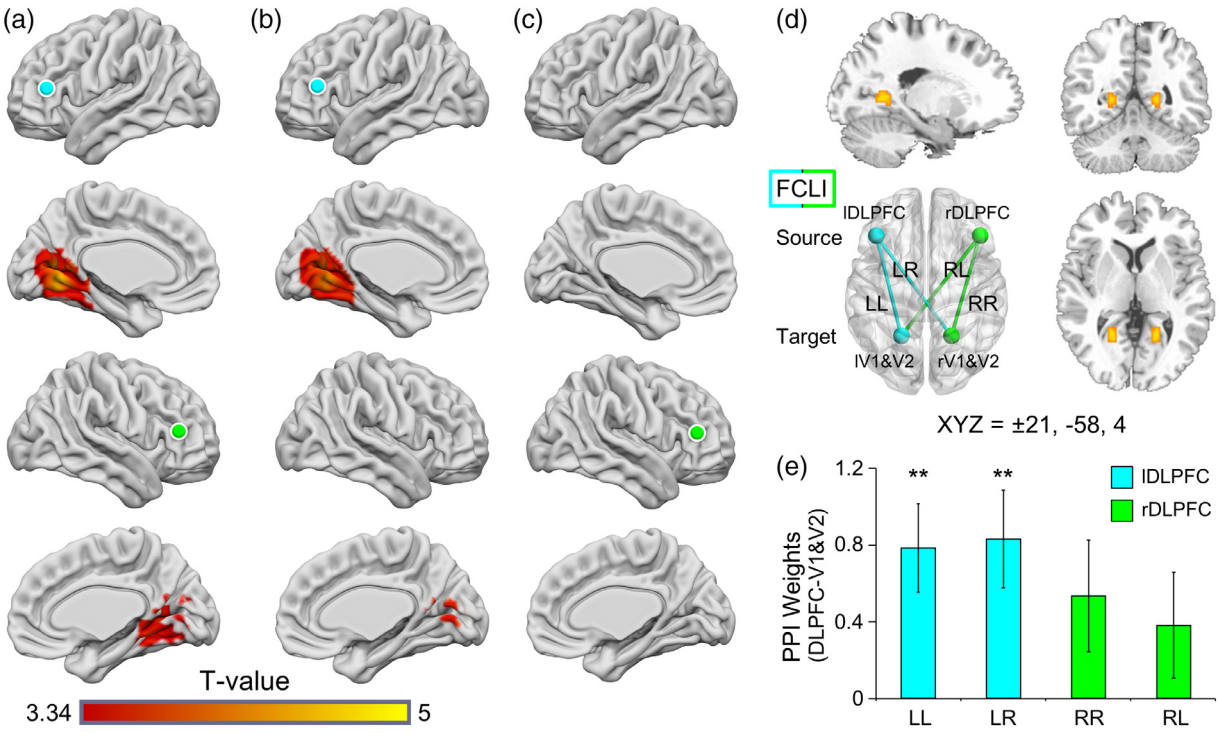

FIGURE 4 The psychophysiological interaction (PPI) and functional connectivity lateralization index (FCLI) regions of bilateral DLPFCs during Stroop task. (a) The total PPI effects of bilateral DLPFCs; (b) the PPI results of left DLPFC; (c) the PPI results of right DLPFC; (d) the FCLI map showed the DLPFC's interactions with other cerebral regions had left lateralization in visual areas V1 and V2. Note that, because of the FCLI algorithm, the results were hemispherical mirrored. The positive FCLI meant the DLPFC's interaction with V1 and V2 was left lateralized. (e) The bars show each lateral DLPFC's averaged PPI beta weights (i.e., 1.13 and 0.67 for lDLPFC and rDLPFC, respectively) in the 6 mm radius spherical ROIs of bilateral V1 and V2 (MNI coordinate: ±21, −58, 1). The error bar shows the 95% confidence interval (CI), that is, lower bound 0.90 and upper bound 1.36 for lDLPFC and lower bound 0.44 and upper bound 0.90 for rDLPFC, respectively (Cousineau, 2005) [Color figure can be viewed at wileyonlinelibrary.com]

TABLE 4 The PPIs and FCLI regions of bilateral DLPFCs during Stroop task

Region	BA	No. voxels	Peak *t*-value	*x*	*y*	*z*
DLPFC total effects						
Lingual/cuneus/posterior cingulate	19/30/18	601	5.37	−9	−61	−5
LDLPFC						
L. Lingual/cuneus/posterior cingulate gyrus	19/30/18	236	4.79	−12	−61	−5
RDLPFC						
FCLI:LDLPFC vs. RDLPFC						
L. Lingual gyrus	30/18	18	3.86	−21	−58	4

respond to Stroop and flanker interferences, which suggest that the conflict detection and task representation are task-general functions of cognitive control. On the other hand, the higher lDLPFC activation of Stroop task than that of flanker task suggests that the greater involvement of the lDLPFC in processing the word-verbal information during the Stroop interference (Hugdahl & Davidson, 2004; Ye & Zhou, 2009). Therefore, although the DLPFC's regulation of task performance is also generally involved in various cognitive control tasks, it is more likely to be a task-dependent component of cognitive control (Braver et al., 2009; Cole et al., 2013). In brief, when facing changing cognitive control situations, the brain needs both stable and flexible substrates for adaptive cognitive control. In the next paragraphs, we would further discuss how the relevant information on task-dependent cognitive control is flexibly represented in the human brain.

The asymmetric activity map of Stroop interference revealed hemodynamic lateralization in the left hemispheric DLPFC, PPC, and temporal lobe. As the language is involved in both the word reading and color naming of Stroop stimuli (Chlebus et al., 2007; January, Trueswell, & Thompson-Schill, 2009; Ye & Zhou, 2009), the asymmetric activation of lDLPFC may be due to lDLPFC's ipsilateral control to language processing that is also left lateralized in the brain. Interestingly, previous studies on the FCA activity of Stroop task showed that when Stroop stimuli were presented in the right visual field, the Stroop effect was larger than that when they were presented in the left visual field (Schmit & Davis, 1974; Tsao, Feustel, & Soseos, 1979). Because the stimuli in one (left or right) visual field were mapped to the contralateral hemisphere, these findings indicated that processing in the left hemisphere induced more language-related interference than the right hemisphere (Belanger & Cimino, 2002; MacLeod, 1991). Thus, the lateral activation in the lDLPFC may suggest that the left DLPFC involve more in controlling the language-related interference through inhibiting task-irrelevant wording reading and/or amplifying task-relevant color naming processing.

In contrast, the asymmetric activation of flanker task was observed in the right aI and fO and right dACC and pSMA suggested that the detection and representation to the visuospatial flanker interference may mainly locate in the right control system (Botvinick et al., 2004; Cole & Schneider, 2007). Previous studies showed the visuospatial attention network is right hemilateral (Corbetta & Shulman,

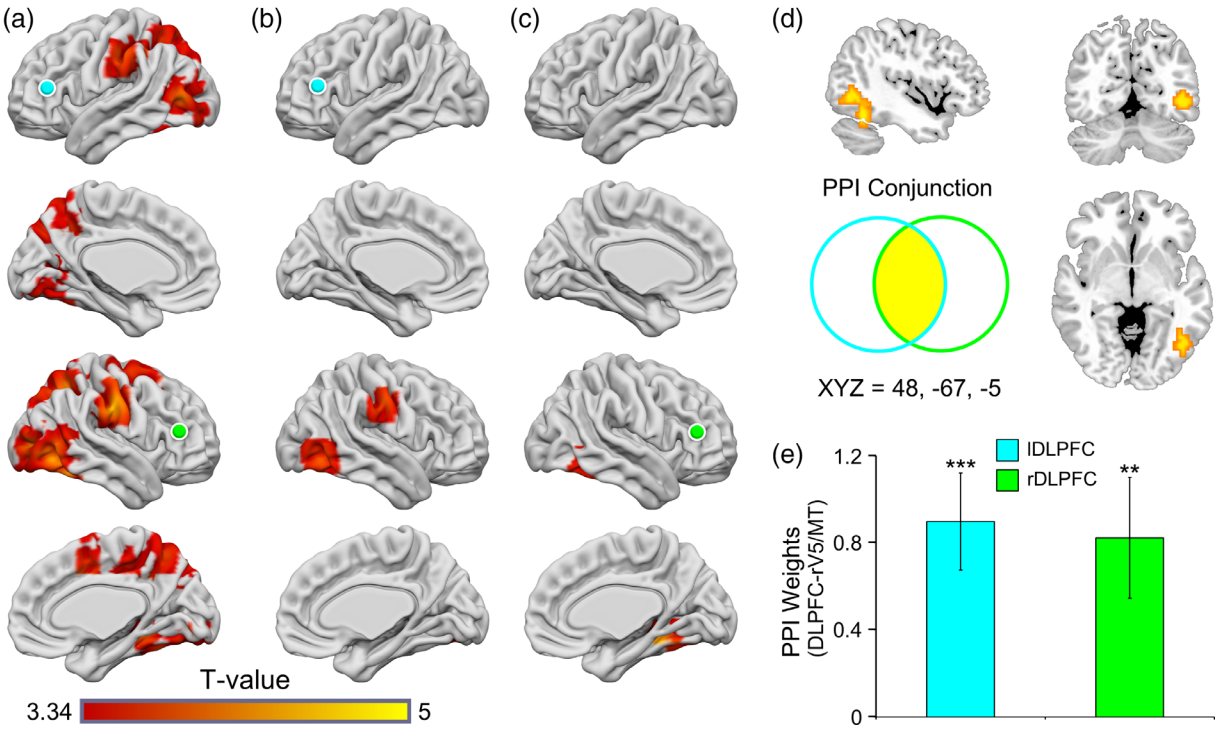

FIGURE 5 The PPI and conjunct PPI results of bilateral DLPFCs during flanker task. (a) The total PPI effects of bilateral DLPFCs; (b) the PPI results of left DLPFC; (c) the PPI results of right DLPFC; (d) the positive conjunct PPIs of bilateral DLPFCs in right V5/MT (BA 37), in this result, a more lenient threshold (voxel-wise $p < .005$ and cluster-wise FWE $p < .05$) was used for display purposes. (e) Each lateral DLPFC's averaged PPI beta weights (i.e., 0.90 and 0.82 for lDLPFC and rDLPFC, respectively) in right V5/MT (6 mm radius spherical ROI, MNI coordinates, 48, −67, −5), the error bar shows the CI (i.e., lower bound 0.61 and upper bound 1.18 for lDLPFC and lower bound 0.54 and upper bound 1.10 for rDLPFC, respectively) (Cousineau, 2005) [Color figure can be viewed at wileyonlinelibrary.com]

TABLE 5 The PPI and conjunct PPI regions of bilateral DLPFCs during flanker task

Region	BA	No. voxels	Peak *t*-value	*x*	*y*	*z*
DLPFC total effects						
R. Superior/middle frontal gyrus	6	148	4.16	24	−4	64
R. Precentral/postcentral gyrus	4/2/3/6	280	5.24	63	−16	40
L. Precuneus/inferior/superior parietal lobule	7/40	376	4.65	−21	−55	49
R. Precuneus/superior parietal lobule	7	365	4.87	24	−55	52
L. Middle occipital/temporal gyrus	19/39/37	352	4.61	−51	−73	7
R. Middle occipital/temporal/fusiform gyrus	19/37	762	5.33	36	−46	−8
LDLPFC						
R. Precentral/postcentral gyrus	4/6	38	4.56	66	−19	37
R. Middle occipital/inferior temporal gyrus	37/19	69	4.35	51	−67	−8
RDLPFC						
R. Middle temporal/fusiform gyrus	19	45	4.87	33	−46	−5
Conjunction: LDLPFC and RDLPFC						
R. Fusiform/inferior temporal gyrus	37	10	3.48	45	−58	−23

2011; Shulman et al., 2010). Because the flanker stimuli we used were directional arrows with visuospatial information, this may result in the cognitive control-related cerebral asymmetries in the right aI and fO and right dACC and pSMA to detect and represent the visuospatial conflict in flanker task (Cornette et al., 1998; Shulman et al., 2010). Besides, none of the corrected asymmetric regions was found in the DLPFC, suggesting the DLPFC may be more symmetric activated when resolving the flanker interference than handling the Stroop task.

To summarize the activation results for flexible cognitive control representation, it is well known that the language processing, which is involved in the Stroop effect, significantly impacts the FCA activity (January et al., 2009; Ye & Zhou, 2009). Through adopting the flanker task, where the arrow direction was language-free, we observed the different FCA activity between these tasks, thus demonstrating that as a general function of cognitive control, the DLPFC flexibly changed its activation patterns to handle various task demands. Nevertheless, since the Stroop and flanker tasks have different stimulus features, to further understand how the human brain efficiently implements the flexible cognitive control. The task-specific processes of the DLPFC should also be reflected in its modulation on other cognitive processes.

As a top-down goal-directed function, the task-dependent inter-regional interactions from the DLPFC to other brain regions were considered through PPI analyses. The results showed that the DLPFC positively interacted with visual areas V1 and V2 for the Stroop task while positively interacted with V5/MT for the flanker task, indicating the task-specific neural mechanisms of the DLPFC to the stimulus processing (Gazzaley et al., 2007; Miller & Cohen, 2001; Zanto, Rubens, Thangavel, & Gazzaley, 2011). Specifically, the positive interactions indicated the DLPFC reallocated more attention to color perception in visual areas V1 and V2 during the Stroop interference than congruent condition (Miceli et al., 2001; Simmons et al., 2007); and also indicated the DLPFC's top–down modulation on the direction processing in the flanker task, since the V5/MT is involved in the perception to motion and direction (Corbetta & Shulman, 2002; Cornette et al., 1998). As a general cognitive function, the control system showed the DLPFC's top-down modulation on the stimulus processing in both tasks. While taking the cognitive control as a flexible cognitive function, our findings refined the neural mechanism of DLPFC as its flexible modulation on task-specific stimulus processes during various cognitive control demands. In addition, since the flanker task was related with the visuospatial stimulus–response mapping, during the control to the flanker interference, the DLPFC's modulation on the PPC and precuneus may respond to the spatial mental imagery (Cavanna & Trimble, 2006), and the DLPFC's modulation on the SMA and primary motor cortex may serve for the spatial response control (Nachev, Kennard, & Husain, 2008).

Furthermore, through calculating the asymmetric PPIs, the different FCLI results between Stroop and flanker tasks further revealed the flexible roles of DLPFC in cognitive control. For the Stroop task, the FCLI and ROI analyses of the PPI signal showed that the lDLPFC had significantly more positive interactions in the V1 and V2 than the rDLPFC under the interference context. While for the flanker task, both the bilateral DLPFCs significantly and positively interacted with right V5/MT and did not show a significant FCLI of PPIs. Thus, the lDLPFC was more inclined to regulate the color feature processing than the rDLPFC during the Stroop task, while both lateral DLPFCs reallocated attention and cognitive resources to the target direction during the flanker task (Chadick & Gazzaley, 2011; Zanto et al., 2011). These results suggested the Stroop task tended to have lateralized PPIs of DLPFC in the verbal color feature domain, while the flanker task tended to have symmetric PPIs of DLPFC in the spatial direction feature domain. This kind of top-down modulation could be further illustrated by the significance level of the edges between the DLPFC and visual cortex in the FCLI analysis. As we see in the Figure 4d, for the lDLPFC source both the lV1 and V2 and rV1 and V2 targets showed significant PPI weights, but none for the rDLPFC source. Correspondingly, neither the lV1 and V2 nor the rV1 and V2 showed significant PPI with both sides of the DLPFC. These findings indicated that it was the DLPFC rather than the visual cortex that played a flexible role in the PPI and top-down cognitive control. Of note, our findings just focused on functional differences between bilateral DLPFCs, but did not deny their common functions during the cognitive control. Taken together, the DLPFC's lateralization of task-specific modulation

in the stimulus perception level further indicated how the human brain implements its flexible cognitive control.

In conclusion, as a general cognitive function, the adaptability of cognitive control is not elusive, it relies on a variety of certainties (e.g., the flexibility). As being revealed in present study, the control system implements its adaptive cognitive control across variety task demands through both task-general salience detection and task-specific goal-directed regulation. These novel findings further clarify the neural mechanisms beneath the cognitive control and suggest the combination of FCA and PPI is a promising method in exploring cognitive control neural mechanisms.

ACKNOWLEDGMENTS

A.C. was supported by the National Natural Science Foundation of China (61431013). Z.C. was supported by the Research Foundation of Jiangxi University of Traditional Chinese Medicine (5151700708). The authors declare no competing financial interests.

ORCID

Antao Chen https://orcid.org/0000-0001-9321-681X

REFERENCES

Bandettini, P. A., & Cox, R. W. (2000). Event-related fMRI contrast when using constant interstimulus interval: Theory and experiment. *Magnetic Resonance in Medicine*, *43*, 540–548.

Belanger, H. G., & Cimino, C. R. (2002). The lateralized stroop: A meta-analysis and its implications for models of semantic processing. *Brain and Language*, *83*, 384–402.

Botvinick, M. M., Braver, T. S., Barch, D. M., Carter, C. S., & Cohen, J. D. (2001). Conflict monitoring and cognitive control. *Psychological Review*, *108*, 624–652.

Botvinick, M. M., Cohen, J. D., & Carter, C. S. (2004). Conflict monitoring and anterior cingulate cortex: An update. *Trends in Cognitive Sciences*, *8*, 539–546.

Brass, M., Ullsperger, M., Knoesche, T. R., Cramon, D. Y.v., & Phillips, N. A. (2005). Who comes first? The role of the prefrontal and parietal cortex in cognitive control. *The Journal of Neuroscience*, *17*, 1367–1375.

Braun, U., Schäfer, A., Walter, H., Erk, S., Romanczuk-Seiferth, N., Haddad, L., … Bassett, D. S. (2015). Dynamic reconfiguration of frontal brain networks during executive cognition in humans. *Proceedings of the National Academy of Sciences of the United States of America*, *112*, 11678–11683.

Braver, T. S., Paxton, J. L., Locke, H. S., & Barch, D. M. (2009). Flexible neural mechanisms of cognitive control within human prefrontal cortex. *Proceedings of the National Academy of Sciences of the United States of America*, *106*, 7351–7356.

Bressler, S. L., & Menon, V. (2010). Large-scale brain networks in cognition: Emerging methods and principles. *Trends in Cognitive Sciences*, *14*, 277–290.

Buckner, R. L., & Vincent, J. L. (2007). Unrest at rest: Default activity and spontaneous network correlations. *NeuroImage*, *37*, 1091–1096.

Carter, C. S., Macdonald, A. M., Botvinick, M., Ross, L. L., Stenger, V. A., Noll, D., & Cohen, J. D. (2000). Parsing executive processes: Strategic vs. evaluative functions of the anterior cingulate cortex. *Proceedings of the National Academy of Sciences of the United States of America*, *97*, 1944–1948.

Cavanna, A. E., & Trimble, M. R. (2006). The precuneus: A review of its functional anatomy and behavioural correlates. *Brain*, *129*, 564–583.

Chadick, J. Z., & Gazzaley, A. (2011). Differential coupling of visual cortex with default or frontal-parietal network based on goals. *Nature Neuroscience*, *14*, 830–832.

Chen, Z., Lei, X., Ding, C., Li, H., & Chen, A. (2013). The neural mechanisms of semantic and response conflicts: An fMRI study of practice-related effects in the Stroop task. *NeuroImage*, *66*, 577–584.

Chlebus, P., Mikl, M., Brázdil, M., Pažourková, M., Krupa, P., & Rektor, I. (2007). fMRI evaluation of hemispheric language dominance using various methods of laterality index calculation. *Experimental Brain Research*, *179*, 365–374.

Cieslik, E. C., Mueller, V. I., Eickhoff, C. R., Langner, R., & Eickhoff, S. B. (2015). Three key regions for supervisory attentional control: Evidence from neuroimaging meta-analyses. *Neuroscience & Biobehavioral Reviews*, *48*, 22–34.

Cocchi, L., Halford, G. S., Zalesky, A., Harding, I. H., Ramm, B. J., Cutmore, T., … Mattingley, J. B. (2013). Complexity in relational processing predicts changes in functional brain network dynamics. *Cerebral Cortex*, *24*, 2283–2296.

Cocchi, L., Zalesky, A., Fornito, A., & Mattingley, J. B. (2013). Dynamic cooperation and competition between brain systems during cognitive control. *Trends in Cognitive Sciences*, *17*, 493–501.

Cole, M. W., Reynolds, J. R., Power, J. D., Repovs, G., Anticevic, A., & Braver, T. S. (2013). Multi-task connectivity reveals flexible hubs for adaptive task control. *Nature Neuroscience*, *16*, 1348–1355.

Cole, M. W., & Schneider, W. (2007). The cognitive control network: Integrated cortical regions with dissociable functions. *NeuroImage*, *37*, 343–360.

Corbetta, M., & Shulman, G. L. (2002). Control of goal-directed and stimulus-driven attention in the brain. *Nature Reviews. Neuroscience*, *3*, 201–215.

Corbetta, M., & Shulman, G. L. (2011). Spatial neglect and attention networks. *Annual Review of Neuroscience*, *34*, 569–599.

Cornette, L., Dupont, P., Rosier, A., Sunaert, S., Van Hecke, P., Michiels, J., … Orban, G. A. (1998). Human brain regions involved in direction discrimination. *Journal of Neurophysiology*, *79*, 2749–2765.

Cousineau, D. (2005). Confidence intervals in within-subject designs: A simpler solution to Loftus and Masson's method. *Tutorial in Quantitative Methods for Psychology*, *1*, 42–45.

De Houwer, J. (2003). On the role of stimulus-response and stimulus-stimulus compatibility in the Stroop effect. *Memory & Cognition*, *31*, 353–359.

Di, X., Kim, E. H., Chen, P., & Biswal, B. B. (2014). Lateralized resting-state functional connectivity in the task-positive and task-negative networks. *Brain Connectivity*, *4*, 641–648.

Dosenbach, N. U., Fair, D. A., Cohen, A. L., Schlaggar, B. L., & Petersen, S. E. (2008). A dual-networks architecture of top-down control. *Trends in Cognitive Sciences*, *12*, 99–105.

Dosenbach, N. U., Visscher, K. M., Palmer, E. D., Miezin, F. M., Wenger, K. K., Kang, H. C., … Petersen, S. E. (2006). A core system for the implementation of task sets. *Neuron*, *50*, 799–812.

Dunst, B., Benedek, M., Koschutnig, K., Jauk, E., & Neubauer, A. C. (2014). Sex differences in the IQ-white matter microstructure relationship: A DTI study. *Brain and Cognition*, *91*, 71–78.

Eckert, M. A., Menon, V., Walczak, A., Ahlstrom, J., Denslow, S., Horwitz, A., & Dubno, J. R. (2009). At the heart of the ventral attention system: The right anterior insula. *Human Brain Mapping*, *30*, 2530–2541.

Egner, T., & Hirsch, J. (2005). Cognitive control mechanisms resolve conflict through cortical amplification of task-relevant information. *Nature Neuroscience*, *8*, 1784–1790.

Eriksen, B. A., & Eriksen, C. W. (1974). Effects of noise letters upon the identification of a target letter in a nonsearch task. *Perception & Psychophysics*, *16*, 143–149.

Fan, J. (2014). An information theory account of cognitive control. *Frontiers in Human Neuroscience*, *8*, 680.

Fan, J., Hof, P. R., Guise, K. G., Fossella, J. A., & Posner, M. I. (2008). The functional integration of the anterior cingulate cortex during conflict processing. *Cerebral Cortex*, *18*, 796–805.

Fan, J., McCandliss, B. D., Fossella, J., Flombaum, J. I., & Posner, M. I. (2005). The activation of attentional networks. *NeuroImage*, *26*, 471–479.

Fan, J., McCandliss, B. D., Sommer, T., Raz, A., & Posner, M. I. (2002). Testing the efficiency and independence of attentional networks. *Journal of Cognitive Neuroscience*, *14*, 340–347.

Fellows, L. K., & Farah, M. J. (2005). Is anterior cingulate cortex necessary for cognitive control? *Brain*, *128*, 788–796.

Forman, S. D., Cohen, J. D., Fitzgerald, M., Eddy, W. F., Mintun, M. A., & Noll, D. C. (1995). Improved assessment of significant activation in functional magnetic resonance imaging (fMRI): Use of a cluster-size threshold. *Magnetic Resonance in Medicine*, *33*, 636–647.

Friston, K. J., Buechel, C., Fink, G. R., Morris, J., Rolls, E., & Dolan, R. J. (1997). Psychophysiological and modulatory interactions in neuroimaging. *NeuroImage*, *6*, 218–229.

Friston, K. J., Holmes, A. P., Worsley, K. J., Poline, J. P., Frith, C. D., & Frackowiak, R. S. (1994). Statistical parametric maps in functional imaging: A general linear approach. *Human Brain Mapping*, *2*, 189–210.

Friston, K. J., Jezzard, P., & Turner, R. (1994). Analysis of functional MRI time-series. *Human Brain Mapping*, *1*, 153–171.

Friston, K. J., Penny, W. D., & Glaser, D. E. (2005). Conjunction revisited. *NeuroImage*, *25*, 661–667.

Friston, K. J., Williams, S., Howard, R., Frackowiak, R. S., & Turner, R. (1996). Movement-related effects in fMRI time-series. *Magnetic Resonance in Medicine*, *35*, 346–355.

Friston, K. J., Worsley, K. J., Frackowiak, R. S., Mazziotta, J. C., & Evans, A. C. (1994). Assessing the significance of focal activations using their spatial extent. *Human Brain Mapping*, *1*, 210–220.

Gazzaley, A., Rissman, J., Cooney, J., Rutman, A., Seibert, T., Clapp, W., & D'Esposito, M. (2007). Functional interactions between prefrontal and visual association cortex contribute to top-down modulation of visual processing. *Cerebral Cortex*, *17*, i125–i135.

Ham, T., Leff, A., de Boissezon, X., Joffe, A., & Sharp, D. J. (2013). Cognitive control and the salience network: An investigation of error processing and effective connectivity. *The Journal of Neuroscience*, *33*, 7091–7098.

Harding, I. H., Yücel, M., Harrison, B. J., Pantelis, C., & Breakspear, M. (2015). Effective connectivity within the frontoparietal control network differentiates cognitive control and working memory. *NeuroImage*, *106*, 144–153.

Hugdahl, K., & Davidson, R. J. (2004). *The asymmetrical brain*. Cambridge, MA: MIT Press.

Hugdahl, K., & Westerhausen, R. (2010). *The two halves of the brain: Information processing in the cerebral hemispheres*. Cambridge, MA: MIT Press.

January, D., Trueswell, J. C., & Thompson-Schill, S. L. (2009). Co-localization of stroop and syntactic ambiguity resolution in Broca's area: Implications for the neural basis of sentence processing. *Journal of Cognitive Neuroscience*, *21*, 2434–2444.

Laird, A. R., McMillan, K. M., Lancaster, J. L., Kochunov, P., Turkeltaub, P. E., Pardo, J. V., & Fox, P. T. (2005). A comparison of label-based review and ALE meta-analysis in the Stroop task. *Human Brain Mapping*, *25*, 6–21.

Leung, H.-C., Skudlarski, P., Gatenby, J. C., Peterson, B. S., & Gore, J. C. (2000). An event-related functional MRI study of the Stroop color word interference task. *Cerebral Cortex*, *10*, 552–560.

Liu, C., Chen, Z., Wang, T., Tang, D., Hitchman, G., Sun, J., … Chen, A. (2015). Predicting stroop effect from spontaneous neuronal activity: A study of regional homogeneity. *PLoS One*, *10*, e0124405.

MacLeod, C. M. (1991). Half a century of research on the Stroop effect: An integrative review. *Psychological Bulletin*, *109*, 163–203.

Menon, V., & Uddin, L. Q. (2010). Saliency, switching, attention and control: A network model of insula function. *Brain Structure & Function*, *214*, 655–667.

Miceli, G., Fouch, E., Capasso, R., Shelton, J. R., Tomaiuolo, F., & Caramazza, A. (2001). The dissociation of color from form and function knowledge. *Nature Neuroscience*, *4*, 662–667.

Miller, E. K., & Cohen, J. D. (2001). An integrative theory of prefrontal cortex function. *Annual Review of Neuroscience*, *24*, 167–202.

Mylius, V., Ayache, S., Ahdab, R., Farhat, W., Zouari, H., Belke, M., … Timmesfeld, N. (2013). Definition of DLPFC and M1 according to anatomical landmarks for navigated brain stimulation: Inter-rater reliability, accuracy, and influence of gender and age. *NeuroImage*, *78*, 224–232.

Nachev, P., Kennard, C., & Husain, M. (2008). Functional role of the supplementary and pre-supplementary motor areas. *Nature Reviews Neuroscience*, *9*, 856–869.

Nichols, T., Brett, M., Andersson, J., Wager, T., & Poline, J. B. (2005). Valid conjunction inference with the minimum statistic. *NeuroImage*, *25*, 653–660.

O'Reilly, J. X., Woolrich, M. W., Behrens, T. E., Smith, S. M., & Johansen-Berg, H. (2012). Tools of the trade: Psychophysiological interactions and functional connectivity. *Social Cognitive and Affective Neuroscience*, *7*, 604–609.

Sakai, K. (2008). Task set and prefrontal cortex. *Annual Review of Neuroscience*, *31*, 219–245.

Schmit, V., & Davis, R. (1974). The role of hemispheric specialization in the analysis of Stroop stimuli. *Acta Psychologica*, *38*, 149–158.

Schultz, D. H., & Cole, M. W. (2016). Higher intelligence is associated with less task-related brain network reconfiguration. *The Journal of Neuroscience*, *36*, 8551–8561.

Shulman, G. L., Pope, D. L., Astafiev, S. V., McAvoy, M. P., Snyder, A. Z., & Corbetta, M. (2010). Right hemisphere dominance during spatial selective attention and target detection occurs outside the dorsal frontoparietal network. *The Journal of Neuroscience*, *30*, 3640–3651.

Simmons, W. K., Ramjee, V., Beauchamp, M. S., McRae, K., Martin, A., & Barsalou, L. W. (2007). A common neural substrate for perceiving and knowing about color. *Neuropsychologia*, *45*, 2802–2810.

Spagna, A., Mackie, M.-A., & Fan, J. (2015). Supramodal executive control of attention. *Frontiers in Psychology*, *6*, 65.

Stevens, M. C., Calhoun, V. D., & Kiehl, K. A. (2005). Hemispheric differences in hemodynamics elicited by auditory oddball stimuli. *NeuroImage*, *26*, 782–792.

Stroop, J. R. (1935). Studies of interference in serial verbal reactions. *Journal of Experimental Psychology*, *18*, 643–662.

Swanson, N., Eichele, T., Pearlson, G., Kiehl, K., Yu, Q., & Calhoun, V. D. (2011). Lateral differences in the default mode network in healthy controls and patients with schizophrenia. *Human Brain Mapping*, *32*, 654–664.

Tsao, Y.-C., Feustel, T., & Soseos, C. (1979). Stroop interference in the left and right visual fields. *Brain and Language*, *8*, 367–371.

Van Veen, V., & Carter, C. S. (2005). Separating semantic conflict and response conflict in the Stroop task: A functional MRI study. *NeuroImage*, *27*, 497–504.

Wu, T., Dufford, A. J., Egan, L. J., Mackie, M.-A., Chen, C., Yuan, C., … Hof, P. R. (2017). Hick–Hyman law is mediated by the cognitive control network in the brain. *Cerebral Cortex*, *28*, 2267–2282.

Ye, Z., & Zhou, X. (2009). Conflict control during sentence comprehension: fMRI evidence. *NeuroImage*, *48*, 280–290.

Zanto, T. P., Rubens, M. T., Thangavel, A., & Gazzaley, A. (2011). Causal role of the prefrontal cortex in top-down modulation of visual processing and working memory. *Nature Neuroscience*, *14*, 656–661.

How to cite this article: Chen Z, Zhao X, Fan J, Chen A. Functional cerebral asymmetry analyses reveal how the control system implements its flexibility. *Hum Brain Mapp*. 2018;39: 4678–4688. https://doi.org/10.1002/hbm.24313